 DOI: 10.1109/IGARSS47720.2021.9553581

TARGET SCATTERING CHARACTERIZATION IN SAR POLARIMETRY USING MODEL-FREE APPROACHES

Subhadip Dey[1], *Avik Bhattacharya*[1], *Alejandro C. Frery*[2], *Carlos López-Martínez*[3]

[1]Microwave Remote Sensing Lab, Centre of Studies in Resources Engineering,
Indian Institute of Technology Bombay, Mumbai, India
[2]School of Mathematics and Statistics, Victoria University of Wellington, New Zealand
[3]Signal Theory and Communications Department (TSC), Universitat Politécnica de Catalunya (UPC),
Barcelona, Spain

ABSTRACT

Target decomposition methods for polarimetric Synthetic Aperture Radar (PolSAR) data aim at explaining the scattering information. In this regard, several conventional model-based methods use scattering power components to analyze polarimetric SAR data. However, the typical hierarchical process to enumerate power components uses various branching conditions, leading to several limitations. This study uses the 3D Barakat degree of polarization (DoP) to obtain the scattered wave polarization state. We employ the DoP to obtain the even bounce, odd-bounce, and diffuse scattering power components. Besides, we propose a measure of target scattering asymmetry, which is subsequently utilized to obtain the helicity power. All the power components in our approach are roll-invariant and non-negative, and the decomposition preserves the total power. We utilized C-band full polarimetric RADARSAT-2 data to show the effectiveness of the proposed decomposition.

***Index Terms*—** Full Polarimetry, Synthetic Aperture Radar, Target Decomposition, Scattering-type Parameter, Target Characterization

1. INTRODUCTION

Polarimetric SAR decomposition methods follow either model-based or eigenvector approaches. On the one hand, eigenvector approaches capture the set of coherent scattering mechanisms. On the other hand, model-based decompositions presume a set of canonical scatterers within a SAR resolution cell. With these assumptions, they try to fit the coherency or covariance matrix concerning those canonical scatterers.

In this aspect, Freeman and Durden [1] proposed a target reflection symmetry based three-component (F3D: surface, double-bounce, and volume) model-based decomposition technique for incoherent targets. Nevertheless, the assumption of reflection symmetry is often limited to natural targets and seldom holds for human-made structures, including urban areas. To account for such non-reflection symmetric conditions, Yamaguchi et al. [2] introduced the helix scattering model along with the surface, double-bounce and volume components in their four-component (Y4O) decomposition method.

The volume models considered in F3D and Y4O decompositions are limited to specific types of vegetation. In this regard, a model-based decomposition introduced a general canopy model [3] and the other proposed simple modification that ensures that all covariance matrices in the decomposition have non-negative eigenvalues corresponding to physical mechanisms [4]. In a later study, Bhattacharya et al. [5], improved the G4U decomposition. A stochastic distance approach was introduced in [6] to modify the Y4O decomposition. Recently, Ratha et al. [7] proposed a scattering factorization framework for the physical interpretation of target scattering from PolSAR data.

Dey et al. [8] proposed the three-component model-free scattering power decomposition for full (MF3CF) and compact (MF3CC) polarimetric SAR data. In their study, the authors used 3D and 2D Barakat degree of polarization [9], and the elements of the coherency (or covariance) matrix to obtain target scattering-type parameters. These parameters were then used to decompose the total scattered power into even-bounce, odd-bounce, and diffused scattering power components. Unlike the volume scattering power component in conventional model-based decompositions, the scattered wave's depolarized part represents the diffused component. With this formulation, all the scattering power components are roll-invariant and non-negative. However, this three-component model-free power decomposition does not explicitly consider the contribution from asymmetric targets.

Hence, we introduce in this work an asymmetric (or helix) scattering-type parameter and, subsequently, the helix scattering power component that was earlier ignored. Similarly to the three-component decomposition method, each power component of this proposed decomposition technique is guaranteed to be non-negative and roll-invariant.

2. METHODOLOGY

In full polarimetry (FP), the multi-looked Hermitian positive semi-definite 3×3 coherency matrix $\mathbf{T}$ is obtained from the averaged outer product of the target vector $\boldsymbol{k}_P$ (derived using the Pauli basis matrix, Ψ_P) with its conjugate (i.e., $\mathbf{T} = \langle \boldsymbol{k}_P \cdot \boldsymbol{k}_P^{*T} \rangle$). In this study, we utilize the 4×4 real matrix representation to describe the backscattering using the Kennaugh matrix ($\mathbf{K}$).

2.1. 3-component decomposition

For 3-component model-free decomposition, the scattering-type parameter, θ_{FP} that is represented using the elements of the $\mathbf{T}$ matrix in [8], can be equivalently expressed using the elements of the $\mathbf{K}$ matrix as,

$$\theta_{\text{FP}} = \tan^{-1} \frac{4 m_{\text{FP}} K_{11} K_{44}}{K_{44}^2 - (1 + 4 m_{\text{FP}}^2) K_{11}^2} \in [-45^\circ, 45^\circ] \quad (1)$$

where $K_{11} = (T_{11} + T_{22} + T_{33})/2$ and $K_{44} = (-T_{11} + T_{22} + T_{33})/2$. This parameter is, thus, roll-invariant and bounded. Its extreme values represent dihedral (-45°) and trihedral (45°) scatterers.

This target characterization parameter, θ_{FP}, is further utilized to derive 3-component scattering power components using a geometrical factor: $(1 \pm \sin 2\theta_{\text{FP}})$. With this, the three decomposed scattering power components can be represented as odd-bounce (P_s), even-bounce (P_d) and diffused (P_v) scattering power components:

$$P_s = m_{\text{FP}}\, K_{11}\, (1 + \sin 2\theta_{\text{FP}}), \quad (2)$$
$$P_d = m_{\text{FP}}\, K_{11}\, (1 - \sin 2\theta_{\text{FP}}), \text{ and} \quad (3)$$
$$P_v = 2\,(1 - m_{\text{FP}})\, K_{11}, \quad (4)$$

where m_{FP} represents the 3D Barakat degree of polarization which infers the polarized part of the scattered electromagnetic wave. Nonetheless, all these decomposed scattering power components are roll-invariant and the total power ($2\,K_{11}$) is conserved after the decomposition.

2.2. 4-component decomposition

For the 4-component model-free decomposition, we first derive the helix power component P_c (6) by modulating the total polarized power (i.e., $2 m_{\text{FP}} K_{11}$) by the scattering asymmetry parameter, τ_{FP},

$$\tau_{\text{FP}} = \tan^{-1} \frac{|K_{14}|}{K_{11}} \in [0^\circ, 45^\circ]. \quad (5)$$

We then obtain the residual power component (P_r (8)), which is equal to the sum of the helix and the diffused power components subtracted from the total scattered power ($2K_{11}$). This residual power component represents the fraction of the polarized scattering power components. This polarized fractional power is then redistributed among the odd (P_s (9)) and even (P_d (10)) power components using the scattering-type parameter θ_{FP} by a geometrical factor $(1 \pm \sin 2\theta_{\text{FP}})$:

$$P_c = 2 m_{\text{FP}} K_{11} \sin 2\tau_{\text{FP}}, \quad (6)$$
$$P_v = 2(1 - m_{\text{FP}}) K_{11}, \quad (7)$$
$$P_r = 2K_{11} - (P_c + P_v) = 2 m_{\text{FP}} K_{11} (1 - \sin 2\tau_{\text{FP}}), \quad (8)$$
$$P_s = \frac{P_r}{2} (1 + \sin 2\theta_{\text{FP}}), \text{ and} \quad (9)$$
$$P_d = \frac{P_r}{2} (1 - \sin 2\theta_{\text{FP}}). \quad (10)$$

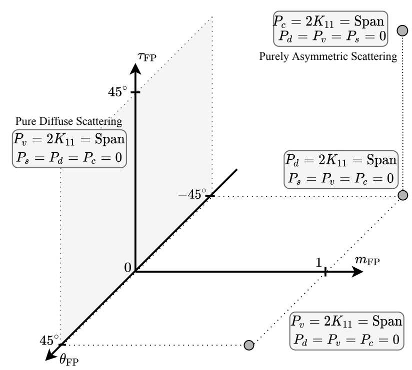

Fig. 1: Scenarios representation with four-scattering powers.

Let us now characterize m_{FP}, θ_{FP} and the four scattering powers for distinct scattering scenarios:

- For a pure diffused scattering-type, i.e., when $m_{\text{FP}} = 0$, then $P_v = 2\,K_{11} = \text{Span}$, and $P_s = P_d = P_c = 0$.
- For polarized scattering types, i.e., when $m_{\text{FP}} = 1$, two cases arise:
  1. if $\theta_{\text{FP}} = 45^\circ$, and $\tau_{\text{FP}} = 0^\circ$, then $P_s = 2\,K_{11} = \text{Span}$, and $P_d = P_v = P_c = 0$.
  2. if $\theta_{\text{FP}} = -45^\circ$, and:
     (a) $\tau_{\text{FP}} = 0^\circ$, then $P_d = 2\,K_{11} = \text{Span}$, and $P_s = P_v = P_c = 0$.
     (b) $\tau_{\text{FP}} = 45^\circ$, then $P_c = 2\,K_{11} = \text{Span}$, and $P_d = P_v = P_s = 0$. In this case, the scattering is purely asymmetric.
- For $\theta_{\text{FP}} = 0^\circ$, i.e., when either $m_{\text{FP}} = 0$, or $K_{44} = 0$, then,
  1. if $m_{\text{FP}} = 0$, and if $\tau_{\text{FP}} = 0^\circ$, then $P_s = P_d = P_c = 0$, and $P_v = 2\,K_{11} = \text{Span}$
  2. if $K_{44} = 0$, and if $\tau_{\text{FP}} = 0^\circ$, then $P_c = 0$ with $P_s = P_d$, and P_v varies with $m_{\text{FP}} \in [0, 1]$

Fig. 1 illustrates these scattering scenarios. The following section discusses the effectiveness of the 3-component and 4-component model-free decompositions over different land-cover types, with C-band full polarimetric RADARSAT-2 data over San-Francisco, CA.

3. RESULTS AND DISCUSSION

The results are shown using a RADARSAT-2 (RS-2) full image over San Francisco (SF), CA, USA. The image is multi-looked with 1 pixel in range and 2 pixels in azimuth directions to generate $10 \times 10\ \mathrm{m}^2$ pixels. Fig. 2 shows the variation of θ_{FP} over ocean ('O'), urban ('U'), oriented urban ('OU') and vegetation ('V') areas. While the medians of O, U and V are well separated, those of OU and U are close as they both denote urban areas. Nonetheless, the values of m_{FP} are low over OU and as a result low θ_{FP} values appears over this area.

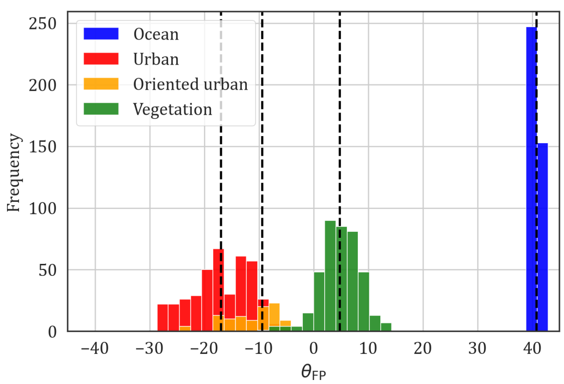

Fig. 2: Variation of θ_{FP} over Ocean, Urban, Oriented urban and Vegetation regions. The dashed vertical line shows the sample median values for each class.

The median values of θ_{FP} over O, U, OU and V are $40.81°$, $-16.856°$, $-9.39°$ and $4.83°$, respectively. The low values of θ_{FP} over V might be due to the equal contribution from regular and irregular parts of canopies.

3.1. 3-component decomposition

Utilizing θ_{FP}, we derive 3-component model-free scattering powers and make a RGB composite for comparison with F3D, as shown in Fig. 3. Fig. 4 shows the power components P_s, P_d and P_v over O, U, OU and V. The dominant scattering powers for O and U are enhanced by $\approx 5\,\%$ to $6\,\%$ wrt F3D.

We observe a significant change for OU. F3D shows high amount of P_v, while MF3CF shows dominant P_v, but significant P_d component. This high P_d is due to the roll-invariant properties of the decomposed power components. Nonetheless, over V, the polarized scattering power components are increased in MF3CF due to the ground-trunk and ground-foliage interaction the EM wave with vegetation canopy.

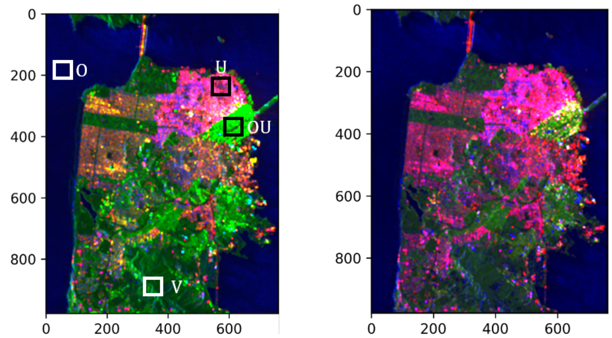

(a) F3D (b) MF3CF

Fig. 3: RGB composite of decomposed power components from (a) F3D and (b) MF3CF techniques. Here: R: P_d, G: P_v and B: P_s

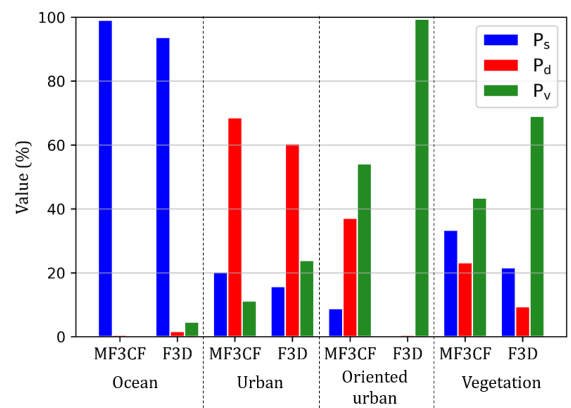

Fig. 4: 3-component scattering power components over ocean, urban, oriented urban and vegetation

3.2. 4-component decomposition

We extended MF3CF to 4-component model-free decomposition (MF4CF) by considering the target asymmetry (τ_{FP}). Fig. 5 shows the variation of τ_{FP} over O, U, OU and V.

It can be seen that τ_{FP} is very low over O ($0.12°$), while over U ($0.72°$) and V ($0.851°$) it is marginally high due to the complex interaction of the EM wave. Over OU, τ_{FP} is higher ($1.79°$) than others due to the orientation effect.

Fig. 6 shows the RGB composites of MF4CF and AG4U. Fig. 7 shows the power components over O, U, OU and V. Similarly to MF3CF, the dominant scattering powers are enhanced over O and U. Besides, a significant change in P_d is observed over OU. Also, the P_c component is increased due to the orientation. As stated before, due to the scattering complexity, a low P_c component is observed over U and V.

4. CONCLUSIONS

We presented model-free scattering power decomposition approaches for full-polarimetric SAR data. We propose

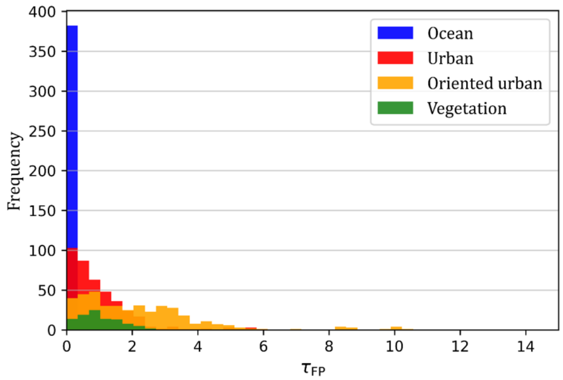

Fig. 5: Variation of τ_{FP} over Ocean, Urban, Oriented urban and Vegetation regions.

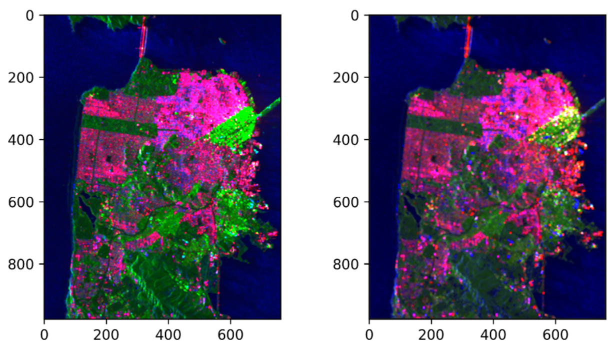

(a) AG4U (b) MF4CF

Fig. 6: RGB composite of decomposed power components from (a) AG4U and (b) MF4CF techniques. Here: R: P_d, G: P_v and B: P_s

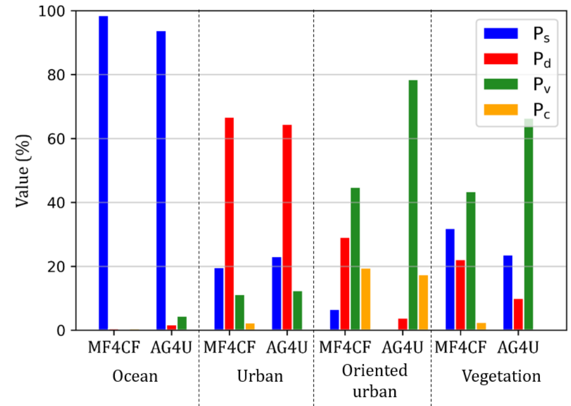

Fig. 7: 4-component scattering power components over ocean, urban, oriented urban and vegetation

the 4-component scattering power decomposition technique (MF4CF) by extending the 3-component technique (MF3CF) using target asymmetry information. Like MF3CF, the overestimation of the volume power component is reduced in MF4CF, while improving the polarized power components. Furthermore, MF4CF produces non-negative power components like MF3CF, which is often a significant drawback of several model-based decompositions. Moreover, the results also show the importance of the asymmetry power component that plays a vital role in discriminating different human-made targets. Thus, these proposed decomposition techniques have good potential for land cover analysis using full polarimetric SAR data.

5. REFERENCES

[1] A. Freeman and S. L. Durden, "A three-component scattering model for polarimetric SAR data," *IEEE Trans. Geosci. Remote Sens.*, vol. 36, no. 3, pp. 963–973, 1998.

[2] Y. Yamaguchi, T. Moriyama, M. Ishido, and H. Yamada, "Four-component scattering model for polarimetric SAR image decomposition," *IEEE Trans. Geosci. Remote Sens.*, vol. 43, no. 8, pp. 1699–1706, 2005.

[3] M. Arii, J. J. van Zyl, and Y. Kim, "A general characterization for polarimetric scattering from vegetation canopies," *IEEE Trans. Geosci. Remote Sens.*, vol. 48, no. 9, pp. 3349–3357, 2010.

[4] J. J. Van Zyl, M. Arii, and Y. Kim, "Model-based decomposition of polarimetric SAR covariance matrices constrained for nonnegative eigenvalues," *IEEE Trans. Geosci. Remote Sens.*, vol. 49, no. 9, pp. 3452–3459, 2011.

[5] A. Bhattacharya, G. Singh, S. Manickam, and Y. Yamaguchi, "An adaptive general four-component scattering power decomposition with unitary transformation of coherency matrix (AG4U)," *IEEE Geosci. Remote Sens. Lett.*, vol. 12, no. 10, pp. 2110–2114, 2015.

[6] A. Bhattacharya, A. Muhuri, S. De, S. Manickam, and A. C. Frery, "Modifying the Yamaguchi four-component decomposition scattering powers using a stochastic distance," *IEEE J. Sel. Topics Appl. Earth Observ. Remote Sens.*, vol. 8, no. 7, pp. 3497–3506, July 2015.

[7] D. Ratha, E. Pottier, A. Bhattacharya, and A. C. Frery, "A polsar scattering power factorization framework and novel roll-invariant parameter-based unsupervised classification scheme using a geodesic distance," *IEEE Trans. Geosci. Remote Sens.*, pp. 1–17, 2019.

[8] S. Dey, A. Bhattacharya, D. Ratha, D. Mandal, and A. C. Frery, "Target characterization and scattering power decomposition for full and compact polarimetric SAR data," *IEEE Trans. Geosci. Remote Sens.*, pp. 1–18, 2020.

[9] R. Barakat, "n-fold polarization measures and associated thermodynamic entropy of N partially coherent pencils of radiation," *Optica Acta: International Journal of Optics*, vol. 30, no. 8, pp. 1171–1182, 1983.